Synchronization of chaos due to linear response in optically driven semiconductor lasers

Atsushi Murakami
Department of Electronic Engineering, The University of Electro-Communications, 1-5-1 Chofu-gaoka, Chofu-shi, Tokyo 182-8585, Japan
(Received 20 August 2001; revised manuscript received 1 March 2002; published 20 May 2002)

This paper presents physical aspects on chaos synchronization in semiconductor lasers (SLs) by studying synchronization from a fundamental standpoint of *driven damped oscillators*. We investigate the simple configuration, a chaotic master SL with optical feedback and a solitary slave SL. The point we emphasize is that the slave laser is regarded as a damped oscillator with relaxation oscillation. Linear stability analysis demonstrates that strong injection can enhance the damping of the slave SL. Consequently, the slave SL can have broad and nearly flat spectral characteristics in its driven response, which is sufficient for covering the broadband chaotic driving signal from the master SL. Numerical simulations verify that the slave SL subject to such strong injection synchronizes well with the chaotic driving signal. We consider that the synchronization phenomenon results from a quasilinear driven response of the slave SL with the remarkable spectral characteristics. Moreover, we discuss this type of chaos synchronization in comparison to anticipating-chaos synchronization occurring in our case from conventional complete synchronization theories, and clarify the different physical aspects of the chaos synchronization scheme. We also show that our analysis agrees well with the earlier experiments that could not have been explained by complete synchronization theory.

DOI: 10.1103/PhysRevE.65.056617 PACS number(s): 05.45.Xt, 42.55.Px, 42.65.Sf

I. INTRODUCTION

Investigating nonlinear systems driven by a time-varying input has been of interest and is related to problems in a wide area of natural and science fields, from chemical, biological, and physiological, to physical systems. In particular, synchronization is an attractive phenomenon in driven nonlinear systems both from a fundamental and an application point of view. Recently, synchronization of nonlinear systems driven with chaotic signals, not by periodic signals, has been a fascinating subject. Several concepts for synchronizing chaos have been suggested, such as complete synchronization [1–3], generalized synchronization [4,5], phase synchronization [6], and lag synchronization [7], and chaos synchronization has been intensively studied in many systems. In particular, lasers have been of great interest due to their potential applications to optical secure communications in which information is conveyed by a chaotic carrier [8–11].

Synchronization of chaotic oscillations in lasers can be easily realized using a simple configuration, consisting of a chaotic master laser and a solitary slave laser coupled by injecting the master laser output into the slave laser. The configuration has been numerically studied in several laser systems, and the synchronized chaos has been well discussed from the standpoint of the conventional complete-synchronization theory [12–15]. The experiment in such a configuration was performed in microchip lasers [16] and semiconductor lasers [17,18], and good synchronization in laser outputs was observed. However, the earlier numerical studies could not explain the observed chaos synchronization very well. There exist some problems in the experimental synchronization, as follows: (i) increasing injection strength realizes much more accurate synchronization [16]; (ii) synchronized chaotic oscillation can be observed even in the presence of large frequency detuning between the two lasers [17,18]. All the authors conclude that the experimentally observed synchronization results from amplification phenomena caused by injection locking in lasers. Moreover, these experimental results verify that synchronization of chaotic outputs in lasers can be easily obtained in asymmetric and mismatched systems, which contradicts the complete-synchronization theories requiring identical or symmetric systems to realize synchronization. Recently, we numerically demonstrated chaos synchronization induced by amplification at a much higher injection level than that previously reported and revealed that the chaos synchronization results from the injection-locking phenomena, which agrees well with the experiments in some aspects [19]. However, there is yet no conclusive explanation of the physics involved, namely, how injection locking can induce such synchronization by amplification.

In this paper, we reconsider the problem from a fundamental standpoint far from the conventional chaos synchronization theories. Since general lasers can be regarded as damped nonlinear oscillators exhibiting damping oscillation, also called ''relaxation oscillation,'' that is a result of an interaction between the complex electric field and the population inversion in the laser cavity. Therefore, we can deal with a case of injecting a master's chaotic output into a solitary slave laser as a fundamental problem of ''*driving damped oscillators*.''

A remarkable feature of driving damped oscillators is *resonance*. If a damped oscillator is driven by a periodic signal very close to the oscillator damping frequency, the oscillator will begin to oscillate at the same frequency as the driving signal but with large amplitude. In contrast, if the driving frequency is far from the damping frequency, the response of the oscillator becomes much smaller compared to the case of resonance. Thus, the oscillator resonance causes a kind of filtering effect. We then consider driving damped oscillators with chaotic signal in the same manner. Because of the broad bandwidth of chaotic signals, the resonance may force damped oscillators to respond by enhancing specific frequency components of a chaotic signal. However,

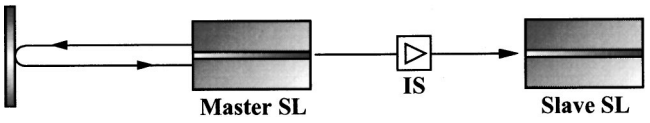

FIG. 1. Configuration of synchronizing coupled semiconductor lasers (SLs). The master SL receives optical feedback from an external reflector and emits feedback-induced chaotic light. The slave SL is driven by unidirectionally injecting the master's chaotic light into the slave's active layer via an optical isolator (IS).

we can also consider that a damped oscillator could synchronize with the chaotic driving signal, if the oscillator could respond linearly to the chaotic drive. ''Linear response'' means that the damped oscillator has a broad bandwidth that sufficiently covers the bandwidth of the chaotic driving signal, has a response even faster than the chaotic time variations, and has an identical gain over the dominant frequency range in the chaotic signal. Such linear-response-induced chaos synchronization may differ considerably from complete synchronization theories.

In this paper, we choose semiconductor lasers and analytically investigate rate equations by performing a linear stability analysis in order to study chaos synchronization in lasers. In particular, we reveal important physical aspects behind synchronization of chaotic oscillations in lasers by taking the standpoint of driven damped oscillators and verify that our analysis can provide a better interpretation of the earlier experiments.

II. MODEL AND RATE EQUATIONS

We consider chaotically driving semiconductor lasers in the simple master-slave configuration depicted in Fig. 1, which is basically the same as the configuration used in the earlier experiments [16–18]. The master laser has an external reflector and exhibits feedback-induced chaotic instabilities. We note that using feedback-induced chaos as a driving signal is very useful for distinguishing the linear-response-induced synchronization (we call this ''linear-amplification-like synchronization'' in the following) from the complete synchronization, discussed later. In order to drive the slave laser, the master chaotic output is unidirectionally injected into the active layer of the slave laser via an optical isolator (IS). Fundamental dynamics, instability, and synchronization in the coupled semiconductor lasers can be described by the following set of rate equations [12–15,19]:

$$\frac{dE_m(t)}{dt}=\frac{1}{2}(1+i\alpha)\{g[N_m(t)-N_0]-\gamma_c\}E_m(t)+\kappa_{\mathrm{ext}}E_m(t-\tau), \tag{1}$$

$$\frac{dE_s(t)}{dt}=\frac{1}{2}(1+i\alpha)\{g[N_s(t)-N_0]-\gamma_c\}E_s(t)+\kappa_{\mathrm{inj}}E_m(t), \tag{2}$$

$$\frac{dN_{m,s}(t)}{dt}=\frac{I_{m,s}}{e}-\gamma_N N_{m,s}(t)-g[N_{m,s}(t)-N_0]|E_{m,s}(t)|^2, \tag{3}$$

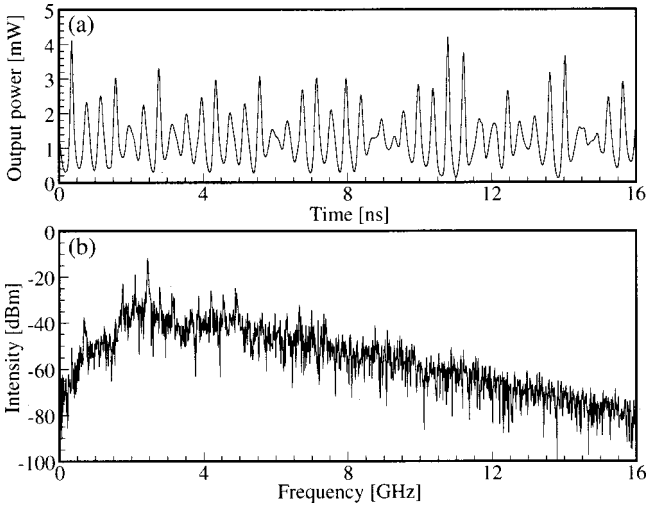

FIG. 2. Typical feedback-induced chaos generated from the master SL. (a) Time series and (b) power spectrum of the master output for the parameters of $I_m=1.3I_{\mathrm{th}}$, $\tau=1$ ns, $r_{\mathrm{ext}}=0.02\%$.

where E and N are the slowly varying complex electric field amplitude and carrier number in the laser cavity, respectively, and the subscripts m and s represent master and slave lasers. Note that the master and slave lasers are assumed to emit at the same optical frequency, namely, no frequency detuning exists between the two lasers. The laser internal parameters are as follows: $\alpha=3$ is the linewidth enhancement factor, $g=7.0\times10^{-6}$ ns^{-1} is the linear gain coefficient, $\gamma_c=518.9$ ns^{-1} is the cavity decay rate, $\gamma_N=0.490$ ns^{-1} is the spontaneous carrier decay rate, I is the pump current, e is the electron charge, and $N_0=1.68\times10^8$ is the carrier number at transparency. τ is the round-trip delay time within the external cavity. Feedback coefficient κ_{ext} is given by $1/\tau_{\mathrm{in}}(1-r_0)\sqrt{r_{\mathrm{ext}}/r_0}$ where τ_{in} is the round-trip time in the laser cavity, and r_0 and r_{ext} represent intensity reflectivity of the laser exit facet and the external reflector ($r_0=0.3$). The coupling strength between the two systems can be given by an injection coefficient κ_{inj} expressed as $1/\tau_{\mathrm{in}}(1-r_0)\sqrt{r_{\mathrm{inj}}/r_0}$ in which r_{inj} represents the injection rate of the master output intensity injected into the slave laser cavity.

We show a typical feedback-induced chaos generated from the master laser in Fig. 2. It results from numerically calculating Eqs. (1) and (3) for variable parameters of the injection current $I_m=1.3I_{\mathrm{th}}$, the feedback delay time $\tau=1$ ns, and the feedback rate $r_{\mathrm{ext}}=0.02\%$ ($\kappa_{\mathrm{ext}}=3.2$ ns^{-1}) by using a fourth-order Runge-Kutta algorithm. These figures present (a) the chaotic time series and (b) its power spectrum. The feedback-induced chaos has a dominant frequency in the gigahertz range corresponding to the relaxation oscillation frequency. Nonlinear mixing between the relaxation oscillation frequency and the external round-trip frequency induced by the external feedback causes a variety of irregularities. The spectrum has a maximum peak around the relaxation oscillation frequency and exhibits broadband characteristics exceeding 10 GHz. We inject this chaotic light into the slave laser in order to realize a chaotic drive. As described in the preceding section, the slave laser must suf-

ficiently cover the bandwidth of the chaotic signal to obtain a linear driven response and the resultant synchronization. In the following section, we perform a linear stability analysis for rate equations and analytically investigate the bandwidth of optically driven semiconductor lasers.

III. LINEAR STABILITY ANALYSIS

We start by presenting rate equations for optically driven semiconductor lasers as a model of the slave laser,

$$\frac{dE(t)}{dt}=\frac{1}{2}(1+i\alpha)\{g[N(t)-N_0]-\gamma_c\}E(t)+\kappa E_{\mathrm{drv}}(t), \tag{4}$$

$$\frac{dN(t)}{dt}=\frac{I}{e}-\gamma_N N(t)-g[N(t)-N_0]|E(t)|^2, \tag{5}$$

where E_{drv} represents the driving optical field amplitude and κ has the same form of κ_{inj}. In Eq. (4), the complex electric field can be divided into amplitude and phase terms assuming $E(t)=A(t)\exp[i\phi(t)]$. Here, the driving field E_{drv} is assumed to be emitted from another semiconductor laser. Since chaotic electric fields emitted from semiconductor lasers are usually modulated in both amplitude and phase, it is appropriate to assume the driving field is modulated in the same way, such as $E_{\mathrm{drv}}(t)=A_{\mathrm{drv}}(t)\exp[i\phi_{\mathrm{drv}}(t)]$. These assumptions yield the following set of three rate equations for the amplitude, the phase, and the carrier number:

$$\frac{dA(t)}{dt}=\frac{1}{2}\{g[N(t)-N_0]-\gamma_c\}A(t)+\kappa A_{\mathrm{drv}}(t)\cos[\phi(t)-\phi_{\mathrm{drv}}(t)], \tag{6}$$

$$\frac{d\phi(t)}{dt}=\frac{\alpha}{2}\{g[N(t)-N_0]-\gamma_c\}-\kappa\frac{A_{\mathrm{drv}}(t)}{A(t)}\sin[\phi(t)-\phi_{\mathrm{drv}}(t)], \tag{7}$$

$$\frac{dN(t)}{dt}=\frac{I}{e}-\gamma_N N(t)-g[N(t)-N_0]A(t)^2. \tag{8}$$

Owing to the optical driving nature, a signal drives the laser on a dc bias component of the injected field. Therefore, dividing the driving-field amplitude into time-constant and time-varying terms, in the form $A_{\mathrm{drv}}(t)=A_{\mathrm{drv},c}+a_{\mathrm{drv}}(t)$, where $A_{\mathrm{drv},c}$ is a constant field amplitude and $a_{\mathrm{drv}}(t)$ represents a signal component, is appropriate to our analysis.

A. Damping oscillation in semiconductor lasers subject to optical injection

First, we investigate the damping oscillation properties of the laser with no signal, i.e., $a_{\mathrm{drv}}=\phi_{\mathrm{drv}}=0$. One can notice that this case is the same as the conventional, well-known optically injected semiconductor lasers with cw light injection, for which a linear stability analysis has already been fully applied [20–23]. Since our analysis follows the previous works, we briefly describe it here. We assume a constant amplitude and phase for the injected field as $A_{\mathrm{drv}}(t)=A_{\mathrm{drv},c}$ and $\phi_{\mathrm{drv}}(t)=\phi_{\mathrm{drv},c}$. From Eqs. (6) to (8), the stationary solutions $A(t)=A_{\mathrm{st}}$, $\phi(t)=\phi_{\mathrm{st}}$, and $N(t)=N_{\mathrm{st}}$ are then given by

$$A_{\mathrm{st}}^2=\frac{I/e-\gamma_N N_{\mathrm{st}}}{g(N_{\mathrm{st}}-N_0)}, \tag{9}$$

$$\Delta\phi_{\mathrm{st}}=\phi_{\mathrm{st}}-\phi_{\mathrm{drv},c}=-\tan^{-1}\alpha, \tag{10}$$

$$N_{\mathrm{st}}=N_0+\frac{\gamma_c-2\kappa A_{\mathrm{st}}\cos\Delta\phi_{\mathrm{st}}}{g}, \tag{11}$$

where we used $A_{\mathrm{drv},c}=A_{\mathrm{st}}$ for the injected field to simplify the analysis. Next, we consider a small perturbation written in the form $x(t)=x_{\mathrm{st}}+\delta x\exp(\lambda t)$ ($x=E$, ϕ, and N), where λ represents a perturbation parameter and is a complex number, in order to investigate the stability of the injected laser. After inserting the small perturbation and the stationary conditions into the rate equations and linearizing the equations, we obtain the following linearized equations for the perturbations in matrix for

$$\begin{pmatrix} \lambda+\kappa\cos\Delta\phi_{\mathrm{st}} & \kappa A_{\mathrm{st}}\sin\Delta\phi_{\mathrm{st}} & -\frac{1}{2}gA_{\mathrm{st}} \\ -\frac{\kappa\sin\Delta\phi_{\mathrm{st}}}{A_{\mathrm{st}}} & \lambda+\kappa\cos\Delta\phi_{\mathrm{st}} & -\frac{\alpha}{2}g \\ 2gA_{\mathrm{st}}(N_{\mathrm{st}}-N_0) & 0 & \lambda+\gamma_N+gA_{\mathrm{st}}^2 \end{pmatrix}\begin{pmatrix}\delta E\\ \delta\phi\\ \delta N\end{pmatrix}=0. \tag{12}$$

A determinant of the coefficient matrix is given by

$$D(\lambda)=\lambda^3+(\gamma_R+2\kappa\cos\Delta\phi_{\mathrm{st}})\lambda^2+(\omega_R^2+\kappa^2+2\kappa\gamma_R\cos\Delta\phi_{\mathrm{st}})\lambda+\kappa^2\gamma_R+\kappa\omega_R^2(\cos\Delta\phi_{\mathrm{st}}-\alpha\sin\Delta\phi_{\mathrm{st}}), \tag{13}$$

where $\omega_R=\sqrt{g\gamma_c A_{\mathrm{st}}^2}$ and $\gamma_R=\gamma_N+gA_{\mathrm{st}}^2$ are the angular frequency and damping rate of relaxation oscillation for the solitary semiconductor laser. In order to establish Eq. (12), the determinant has to be zero, giving a stability condition for the injected lasers. We solve the zeros of D by dividing λ into real and imaginary parts ($\lambda=\gamma+i\omega$) and obtain a linear mode as a pair of γ and ω [24,25]. From the assumed perturbations, the real (imaginary) part of λ represents a damping rate (angular frequency) of the damping oscillation. Therefore, a linear mode with negative γ represents damping oscillation, while a positive γ represents unstable oscillation of the injected lasers. Furthermore, the bandwidth of the injected laser can be determined by the damping oscillation frequency ω.

Figure 3 illustrates a linear mode of the injected laser moving in a phase space of (γ, ω) with change of the optical injection rate r_{inj}. Circles represent the linear modes for different values of r_{inj}, and the gray line represents the locus of the linear mode transition. For $r_{\mathrm{inj}}=0\%$, the linear mode corresponds to the relaxation oscillation of the solitary semi-

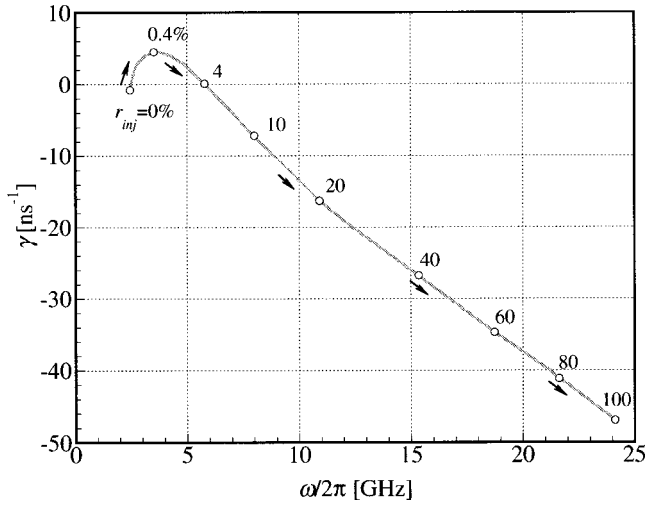

FIG. 3. Transition of linear mode of optically injected semiconductor lasers with increased injection rate r_{inj} obtained from a linear stability analysis. Horizontal and vertical axes represent frequency and damping rate of the linear mode. The arrows denote directions of the mode transition. The gray curve displays locus of the mode transition.

conductor lasers exhibiting damping oscillation with negative γ at a frequency of about 2.5 GHz. With increased injection, the linear mode moves in the direction denoted by arrows. For a weak injection, the mode enters the $\gamma>0$ region, explaining that the laser becomes unstable due to the optical injection itself. Actually, injected lasers in this region are known to exhibit bifurcation routes to chaos [26]. The unstable mode becomes stable again for $r_{\mathrm{inj}}=4\%$. It should be noted that the stable-mode regime corresponds to the injection-locking regime at strong injection level. Further increase of the injection increases both the damping rate and the oscillation frequency of the linear mode. The mode transition explicitly exhibits a bandwidth broadening of the injected laser. We find that, for a high injection rate, the injected laser begins to have a sufficiently broad bandwidth to cover the chaotic driving signal of Fig. 2.

B. Frequency response of driven injected semiconductor lasers

Second, we analyze Eqs. (6) to (8) including the signal term and derive a driven response of the injected laser around the stationary state. We assume the signal term also takes the perturbation form $A_{\mathrm{drv}}(t)=A_{\mathrm{drv},c}+\delta a_{\mathrm{drv}}\exp(\lambda t)$ and $\phi_{\mathrm{drv}}(t)=\phi_{\mathrm{drv},c}+\delta\phi_{\mathrm{drv}}\exp(\lambda t)$ in the same manner as the other variables. Inserting the signal terms with all the other perturbed variables into Eqs. (6) to (8) leads to the following set of linear equations:

$$\lambda\,\delta A=-\kappa\cos\Delta\phi_{\mathrm{st}}\delta A-\kappa A_{\mathrm{st}}\sin\Delta\phi_{\mathrm{st}}\{\delta\phi-\delta\phi_{\mathrm{drv}}\}+\frac{1}{2}gA_{\mathrm{st}}\delta N+\kappa\cos\Delta\phi_{\mathrm{st}}\delta a_{\mathrm{drv}},\tag{14}$$

$$\lambda\,\delta\phi=\frac{\kappa\sin\Delta\phi_{\mathrm{st}}}{A_{\mathrm{st}}}\delta A-\kappa\cos\Delta\phi_{\mathrm{st}}[\delta\phi-\delta\phi_{\mathrm{drv}}]+\frac{\alpha}{2}g\,\delta N-\frac{\kappa\sin\delta\phi_{\mathrm{st}}}{A_{\mathrm{st}}}\delta a_{\mathrm{drv}},\tag{15}$$

$$\lambda\,\delta N=-2gA_{\mathrm{st}}(N_{\mathrm{st}}-N_0)\,\delta A-(\gamma_N+gA_{\mathrm{st}}^2)\,\delta N.\tag{16}$$

Owing to the limitation of linear stability analysis, we cannot investigate the laser-driven response simultaneously for both the amplitude and the phase components of the driving signal. Therefore, we derive a response to the amplitude drive and a response to the phase drive independently. We thus express the driven response in the form of $\delta A/\delta a_{\mathrm{drv}}$ for $\delta\phi_{\mathrm{drv}}=0$ and $\delta\phi/\delta\phi_{\mathrm{drv}}$ for $\delta a_{\mathrm{drv}}=0$. Inserting $\lambda=i\omega$ can lead to their frequency responses. From Eqs. (14) to (16), we obtain

$$\frac{\delta A}{\delta a_{\mathrm{drv}}}=\frac{[\gamma_R\kappa^2-\kappa\cos(\Delta\phi_{\mathrm{st}})\omega^2]+i[\kappa^2+\gamma_R\kappa\cos(\Delta\phi_{\mathrm{st}})]\omega}{D(i\omega)},\tag{17}$$

$$\frac{\delta\phi}{\delta\phi_{\mathrm{drv}}}=\frac{\{\gamma_R\kappa^2+\kappa\omega_R^2[\cos(\Delta\phi_{\mathrm{st}})-\alpha\sin(\Delta\phi_{\mathrm{st}})]-\kappa\cos(\Delta\phi_{\mathrm{st}})\omega^2\}+i[\kappa^2+\gamma_R\kappa\cos(\Delta\phi_{\mathrm{st}})]\omega}{D(i\omega)},\tag{18}$$

where D is the determinant given by Eq. (13). Figure 4 depicts plots of Eqs. (17) and (18) for different injection rates. Figure 4(a) presents the spectrum of the amplitude drive of the injected laser. We find that the spectrum has a resonance peak that corresponds to the damping oscillation mode shown in Fig. 3. The figure demonstrates that the spectral bandwidth becomes much broader with the increased injection rate and that the spectrum structure becomes almost flat with the suppression of the resonance peak. We consider that the resonance suppression is due to enhanced damping of the linear mode, as shown in Fig. 3. A similar tendency is observed for the phase-drive case shown in Fig. 4(b). A remarkable difference is observed between the two spectra. Specifically the gain in the low-frequency region is reduced for the amplitude-drive case but not in the phase-drive case. This means that the injected laser is more likely to provide linear response in the driving phase than in the driving amplitude. However, the analysis almost seems to predict that injected semiconductor lasers with sufficiently high injection can exhibit a linearlike driven response to any broadband driving

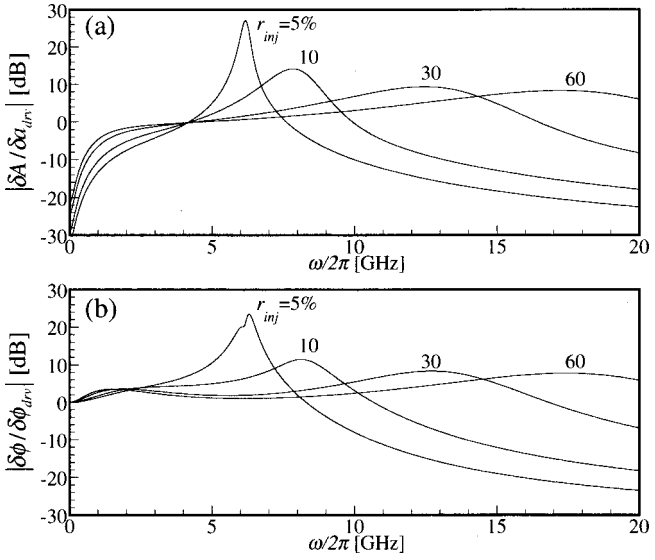

FIG. 4. Spectra of the injected laser showing frequency response to (a) amplitude drive and (b) phase drive for different values of r_{inj}.

signal, either amplitude or phase, if the signal bandwidth is covered within the laser bandwidth.

IV. NUMERICAL ANALYSIS

In this section, we numerically simulate the full rate equations of Eqs. (1)–(3) and examine the above theoretical predictions from the linear stability analysis. We use the master's chaotic state of Fig. 2 as a driving signal and investigate slave laser response for the injection rates $r_{\mathrm{inj}}=5$ and 30%, for each of which the slave laser has an intensive resonance peak at 6 GHz in the response spectrum or has a nearly flat spectrum (see Fig. 4). Note that the values of r_{inj} we use here are comparable to those of the experiment in Refs. [17], [18]. First, we present the result for $r_{\mathrm{inj}}=5\%$ in Fig. 5. Figure 5(a) depicts the time series. The solid curve illustrates the driven response of the slave laser, and the gray line shows the driving chaotic signal of the master laser that is vertically shifted for clear comparison. We find that the slave laser partly follows the driving signal but oscillates at a much higher frequency. We can investigate the slave response in the frequency domain in Fig. 5(b). The solid (gray) line corresponds to the slave (master) laser. These two spectra overlap and are very similar to each other up to about 5 GHz. However, the slave laser amplifies the driving signal too much in the higher frequency range. We consider that the excess amplification is induced by the high resonance around 6 GHz in the spectrum of Fig. 4. Figure 6 presents the result for an even stronger injection of $r_{\mathrm{inj}}=30\%$. Figure 6(a) demonstrates that the slave laser almost exactly follows the driving chaotic signal, realizing chaos synchronization. As shown in Fig. 6(b), the spectra correspond to each other very well up to about 8 GHz. It may be reasonable to consider that this synchronized chaos results from the linear response of the injected laser with the bandwidth broadening. In this case, the effect of the excess amplification for the higher

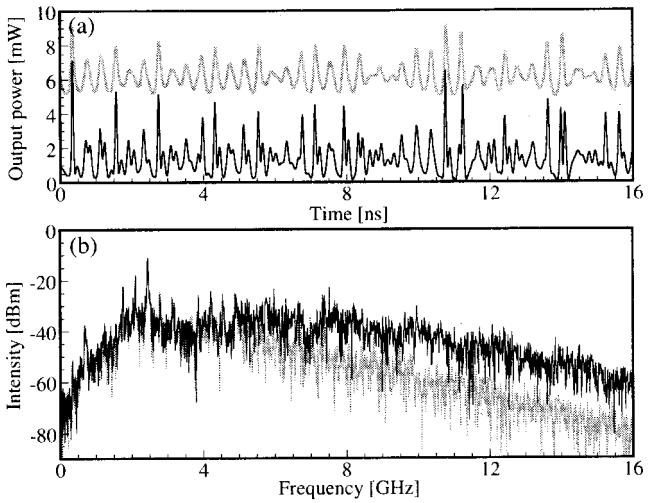

FIG. 5. Numerical result of chaotic driven semiconductor lasers for a weak injection. (a) Driving signal of the master SL (gray line) and response of the slave SL (solid line), and (b) their power spectra. The driving signal is the same as shown in Fig. 2. The weak injection rate is $r_{\mathrm{inj}}=5\%$, and the other parameters are $I_m=I_s=1.3I_{\mathrm{th}}$, $\tau=1$ ns, and $r_{\mathrm{ext}}=0.02\%$.

frequency region is trivial in the synchronized behavior because the signal components in the frequency region are sufficiently small themselves.

As previously shown, the numerical results reflect the analytical predictions. Since chaotic dynamics are generated due to laser nonlinearity, the linear stability analysis does not completely explain chaotically driving lasers. Indeed, the gain reduction of the amplitude-driven response spectrum appearing in the lower frequency region in Fig. 4(a) is not observed in the numerical results. (Note that the spectra of the signal and the driven response correspond well to each other even in the low-frequency range.) However, it is important to notice that our analysis verifies the scenario that

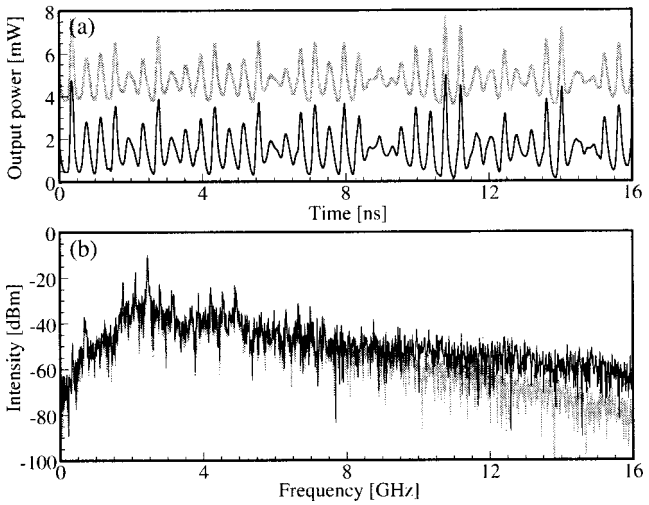

FIG. 6. Well-synchronized chaotic state from the driven response of the slave SL for a strong injection. The injection rate is $r_{\mathrm{inj}}=30\%$, and the other parameter values are identical to those in Fig. 5.

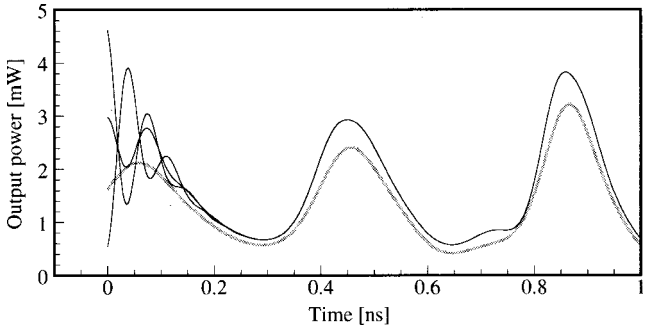

FIG. 7. Stability of synchronization corresponding to the previous result in Fig. 6. The gray line shows the chaotic driving signal of the master SL, and solid lines illustrate time traces of the well-synchronized slave SL from three different perturbations applied at $t=0$. The slave SL rapidly converges to the synchronized state again after the transient relaxation oscillations.

high optical injection can provide semiconductor lasers bandwidth broadening and lead to synchronization of chaos due to the linear response. We should mention that bandwidth broadening induced by strong optical injection in semiconductor lasers (SLs) is not a novel phenomenon, but has already been intensively studied without connection to the chaos synchronization problem [21,22]. It is also important to note that the literature described such bandwidth enhancement of injected lasers as a cavity phenomenon that does not occur in a traveling wave amplifier.

We investigated synchronization stability against perturbation. In the numerical calculation, we moderately deviated the electric field of the slave laser that is in the stable synchronized state, and traced the slave's behavior. We chose the synchronized state of Fig. 6. The result is presented in Fig. 7, in which the gray line is the master's driving signal and the solid lines show the temporal response of the slave laser output after three perturbations are applied at $t=0$. We find that the slave laser converges rapidly to the synchronized state after exhibiting a transient relaxation oscillation within a very short time (<0.2 ns) compared to the chaotic time fluctuations. For this reason, we link the synchronization stability to the damping characteristics of the injected laser shown in Fig. 3. The linear mode analysis has estimated that, for $r_{\mathrm{inj}}=30\%$, the damping rate and frequency are -22.0 ns^{-1} and 13.3 GHz. The damping oscillation period converted in the time domain is then 0.075 ns and agrees well with the transient relaxation oscillation in the numerical result of Fig. 7.

We also investigated the driven response of the slave SL for variations in some system parameters. In order to quantitatively estimate the similarity between the driving signal and the driven response, we calculate a correlation defined as $\sigma=\langle|S_m-S_s|\rangle/\langle S_m\rangle$ where S represents the normalized intensity of the laser output and $\langle\cdots\rangle$ denotes the time average. First, we choose the chaotic driving signal of Fig. 2 and vary the injection rate from 5 to 100%. Figure 8(a) shows the calculated σ as a function of r_{inj}. The value of σ asymptotically decreases as the injection increases because the bandwidth of the slave SL is broadened with the increased injection, and the accuracy of the synchronized response of the

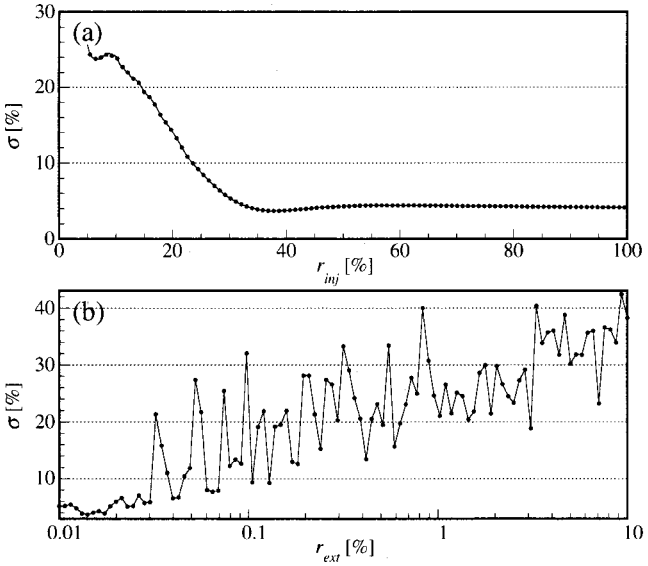

FIG. 8. Synchronization performance versus parameter variations with a correlation σ between the master's chaotic driving signal and the slave's synchronized output. (a) The driving signal is chosen to be Fig. 2 and the injection rate is varied. (b) The injection rate is fixed to $r_{\mathrm{inj}}=30\%$, and the feedback rate is varied.

slave SL increases. This is consistent with the linear mode analysis of Fig. 3 and also agrees well with the experimental result in Ref. [16]. σ reaches a constant value at $r_{\mathrm{inj}}=35\%$. Second, we fix the injection rate to $r_{\mathrm{inj}}=30\%$ and vary the feedback rate of the master SL from 0.01 to 10%. The result is shown in Fig. 8(b) where a log scale is used for the horizontal axis for clarity. The figure demonstrates that the correlation entirely tends to decrease with increasing r_{ext}. We consider that increasing the feedback rate can broaden the master's bandwidth, generating a much-broadened chaotic signal. We interpret this result as meaning that the bandwidth of the chaotic signal becomes larger toward that of the slave SL, decreasing the synchronization ability of the slave SL.

V. DISCUSSION

So far, we have concentrated on the synchronized chaos in semiconductor lasers due to the linearlike response. Here, we show complete synchronization generated in our configuration and discuss physical properties and differences for complete synchronization and linear-amplification-like synchronization. The reason why we have used the feedback-induced chaos as the driving signal is that synchronized states for the two types of synchronization differ considerably. In the conventional theories of complete synchronization, the two synchronized systems have to be symmetric; all the parameters in the two systems have to be the same or equivalent [1–3]. In this situation, the two systems may have mathematically complete synchronous solutions. For example, in our case, the two laser systems can be described by the same, or equivalently the same, rate equation when all the laser parameters are the same, and the feedback strength of the master laser is identical to the injection strength into the slave laser, i.e., $\kappa_{\mathrm{ext}}=\kappa_{\mathrm{inj}}$. Under these conditions, there is a syn-

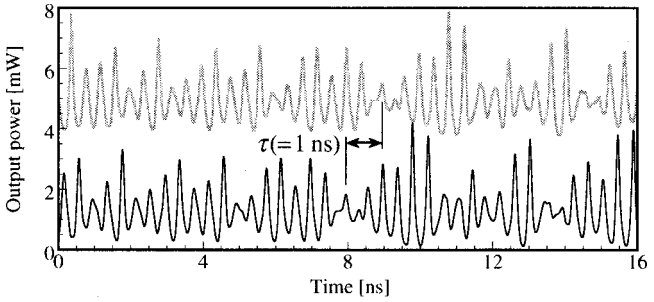

FIG. 9. Anticipating synchronization in our case calculated for the symmetry conditions required by the conventional theories for complete chaos synchronization. Calculation conditions for the complete chaos synchronization are $I_m = I_s = 1.3 I_{\mathrm{th}}$, $\tau = 1$ ns, and $r_{\mathrm{ext}} = r_{\mathrm{inj}} = 0.02\%$. The solid (gray) line corresponds to the slave (master) SL. The slave SL oscillates and anticipates the master's behavior by time τ.

chronous solution, $E_m(t) = E_s(t-\tau)$ [12–15]. The existence of a time shift between the two laser outputs is a remarkable feature in complete synchronization observed in our case. In this time shift, the slave laser anticipates the future state of the master's behavior. The anticipation is known to be a general phenomenon observed in other synchronized time-delay systems [2]. The anticipating synchronization has been the major problem and discrepancy between the theory and the experiment because there was no such time shift in the experimental synchronization. However, we emphasize that our analysis follows the experimental results because here also no such time shift exists in amplificationlike synchronization, as already presented in Fig. 6. Figure 9 shows anticipating synchronization in our case for the driving signal of Fig. 2. In this case, the complete synchronization conditions are $I_m = I_s (= 1.3 I_{\mathrm{th}})$ and $r_{\mathrm{ext}} = r_{\mathrm{inj}} (= 0.02\%)$. The slave laser synchronizes with the driving signal with a time shift corresponding to the feedback delay time ($\tau = 1$ ns) while anticipating the future state of the master's chaotic behavior. Our previous numerical study revealed that this synchronized state is very unstable and is easily broken by including noise or parameter mismatches of even a few percent between the two lasers [19]. It seems difficult to observe such anticipating synchronization in real laser experiments [14].

A remarkable feature of the linear-amplification-like synchronization is the feasibility in asymmetric systems, as clearly demonstrated in Fig. 8(a). Increasing the injection rate alone with respect to the fixed feedback rate drives the slave system farther from symmetry with the master system because the symmetry requirement can be defined as having equal injection and feedback rates. In spite of that, the figure shows that the slave laser becomes well synchronized. We consider that this explains the experimental result of Ref. [16]. Moreover, as was shown in our previous work (in Ref. [19]), the other mismatched parameters do not prevent synchronization. Particularly, linear-amplification-like synchronization can be realized in the wide range of the frequency detuning. This agrees well with the experimental result of Refs. [17], [18].

The conventional theories suggest that the strict symmetry of systems required for successful synchronization can play an important role as a security key in private communications using chaos synchronization because someone with a slightly mismatched receiver cannot get coded information due to the failure in synchronizing the chaotic carrier. In contrast, a kind of linear-amplification-like chaos synchronization in lasers may provide different applications, even in implementing private communications, due to the robustness of synchronization against parameter mismatch. These subjects should be discussed in other literature.

We mention that the linear-amplification-like synchronization can be considered a kind of phase synchronization because the main physical cause comes from injection locking that includes ''phase-locking'' phenomena. Indeed, good synchronization is observed in phase fluctuations in the synchronized state of Fig. 6. Moreover, in Fig. 5, phases are well synchronized, even though the field amplitudes (or intensities) are not synchronized. However, the conventional phase-synchronization scheme, coupling method considerably differs, in that the coupling between two systems is realized in taking difference of their outputs in many studies [6]. In our configuration, only the master laser's complex field amplitude is unidirectionally coupled into the slave laser due to optical manner. Therefore, we consider that further discussion would be needed in directly classifying the linear-amplification-like synchronization into the conventional phase synchronization.

VI. CONCLUSION

We have theoretically studied chaos synchronization in coupled semiconductor lasers from the viewpoint of driven damped oscillators, and, as a result, obtained a good explanation of why one can observe a linear-amplification-like synchronized chaos in experiments. In our system, a chaotic light signal generated from a semiconductor laser with optical feedback can drive another semiconductor laser in a master-slave configuration in which the two lasers are coupled by unidirectionally injecting the master laser output into the slave laser. The driven laser is always subjected to a constant-intensity bias field injection in the absence of the driving signal. This bias field injection can induce a major change in the damping properties of the laser as a damped oscillator.

We performed a linear stability analysis and analytically demonstrated that increasing injection can increase the frequency and damping rate of the damping oscillation in constant-intensity-injected semiconductor lasers. This can lead to a bandwidth broadening for the injected semiconductor laser. We also applied the analysis to the case with a driving signal and derived a spectral characteristic of the driven laser as a function of driving frequency. The linear stability analysis predicted that a semiconductor laser with optical injection can exhibit a linearlike driven response to broadband driving signals under strong injection; the linear response was characterized by a nearly flat spectral shape resulting from the bandwidth broadening of the injected laser and from the suppression of the resonance peak in the spectrum by enhanced damping.

We examined these analytical results by numerically

simulating the full set of rate equations in our system. We chose a broadband chaotic signal in a tens-of-gigahertz range generated from the master laser with optical feedback, and investigated the response of the driven slave laser for weak and strong optical injection. For weak injection, we confirmed that the effective resonance of the slave laser enhances and amplifies the frequency part of the driving signal corresponding to the resonance frequency and its neighborhood, degrading synchronization. In contrast, strong injection suppresses the resonance and provides linearlike response to the driven laser. As a result, the numerical simulation explicitly showed that the slave synchronized well with the driving chaotic signal. Synchronization stability was investigated by perturbing the synchronized slave laser. The slave laser rapidly converges to stable synchronization much more quickly than the chaotic fluctuation. We considered that the very fast response results from the enhanced damping of the strongly injected laser and agreed with the linear mode analysis. We calculated a correlation of outputs between the master and slave SLs by varying the feedback rate and injection rate, and confirmed the interrelation of bandwidths between the driving signal and the slave SL with respect to synchronization.

We also discussed this linear-amplification-like synchronization with respect to the conventional theory of complete synchronization. Our synchronizing system also possesses a complete synchronous solution in a mathematical sense. These two types of synchronization can be clearly distinguished from each other by the existence or absence of a time shift between the driving signal and synchronized chaos. The time shift always occurs in the conventional theory of complete synchronization in synchronized time-delay systems but does not occurs in the amplification case. We discussed differences and characteristics of both cases from the relation between synchronization and system parameter mismatches, and emphasized the feasibility in asymmetric systems as a remarkable feature of linear-response-induced chaos synchronization. We mention that the linear-amplification-like synchronization can be considered a kind of phase synchronization.

We conclude that the controversial experimental synchronization in lasers results from the linear-like-amplification with the enhanced damping and the bandwidth broadening induced by the strong optical injection, but not from the complete-synchronization theory. Particularly, our analysis verified to provide a good interpretation of the experimental chaos synchronization in semiconductor lasers with optical feedback that can be observed in the absence of the anticipating time shift and in variation of injection level within the strong injection-locking regime.

ACKNOWLEDGMENT

Valuable support by Professor K. Atsuki in conducting the investigations is gratefully acknowledged.

[1] L. M. Pecora and T. L. Carroll, Phys. Rev. Lett. **64**, 821 (1990); Phys. Rev. A **44**, 2374 (1991).
[2] K. Pyragas, Phys. Lett. A **181**, 203 (1993); Phys. Rev. E **58**, 3067 (1998); H. U. Voss, *ibid.* **61**, 5115 (2000).
[3] L. Kocarev and U. Parlitz, Phys. Rev. Lett. **19**, 5028 (1995).
[4] N. F. Rulkov, M. M. Sushchik, L. S. Tsimring, and H. D. I. Abarbanel, Phys. Rev. E **51**, 980 (1995).
[5] L. Kocarev and U. Parlitz, Phys. Rev. Lett. **76**, 1816 (1996).
[6] M. G. Rosenblum, A. S. Pikovsky, and J. Kurths, Phys. Rev. Lett. **76**, 1804 (1996).
[7] M. G. Rosenblum, A. S. Pikovsky, and J. Kurths, Phys. Rev. Lett. **78**, 4193 (1997).
[8] P. Colet and R. Roy, Opt. Lett. **19**, 2056 (1994).
[9] C. R. Mirasso, P. Colet, and P. Garcia-Fernandez, IEEE Photonics Technol. Lett. **8**, 299 (1996); A. Sanchez-Diaz, C. R. Mirasso, P. Colet, and P. G-Fernandez, IEEE J. Quantum Electron. **35**, 292 (1999).
[10] G. D. Van Wiggeren and R. Roy, Science **279**, 1198 (1998); Phys. Rev. Lett. **81**, 3547 (1998).
[11] J.-P. Goedgebuer, L. Larger, and H. Porte, Phys. Rev. Lett. **80**, 2249 (1998).
[12] V. Ahlers, U. Parlitz, and W. Lauterborn, Phys. Rev. E **58**, 7208 (1998).
[13] A. Murakami and J. Ohtsubo, Phys. Rev. E **63**, 066203 (2001).
[14] Y. Liu, H. F. Chen, J. M. Liu, P. Davis, and T. Aida, Phys. Rev. A **63**, 031802(R) (2001).
[15] C. Masoller, Phys. Rev. Lett. **86**, 2782 (2001).
[16] A. Uchida, T. Ogawa, M. Shinozuka, and F. Kannari, Phys. Rev. E **62**, 1 (2000).
[17] Y. Takiguchi, H. Fujino, and J. Ohtsubo, Opt. Lett. **24**, 1570 (1999); H. Fujino and J. Ohtsubo, *ibid.* **25**, 625 (2000).
[18] I. Fischer, Y. Liu, and P. Davis, Phys. Rev. A **62**, 011801(R) (2000).
[19] A. Murakami and J. Ohtsubo, Phys. Rev. A **65**, 033826 (2002).
[20] F. Mogensen, H. Olesen, and G. Jacobsen, IEEE J. Quantum Electron. **21**, 784 (1985).
[21] T. B. Simpson, J. M. Liu, and A. Garvrielides, IEEE J. Quantum Electron. **32**, 1456 (1996); T. B. Simpson and J. M. Liu, IEEE Photonics Technol. Lett. **9**, 1322 (1997).
[22] G. Yabre, J. Lightwave Technol. **14**, 2367 (1996).
[23] V. Annovazzi-Lodi, A. Scire, M. Sorel, and S. Donati, IEEE J. Quantum Electron. **34**, 2350 (1998).
[24] Y. Liu, N. Kikuchi, and J. Ohtsubo, Phys. Rev. E **51**, R2697 (1995).
[25] A. Murakami and J. Ohtsubo, IEEE J. Quantum Electron. **34**, 1979 (1998).
[26] V. Kovanis, A. Gavrielides, T. B. Simpson, and J. M. Liu, Appl. Phys. Lett. **67**, 2780 (1995); T. B. Simpson, J. M. Liu, K. F. Huang, and K. Tai, Quantum Semiclassic. Opt. **9**, 765 (1997).